Supporting Information

Microscopic Mechanism of the Helix-to-Layer Transformation in Elemental Group VI Solids

Dan Liu,[1] Xianqing Lin,[1,2] and David Tománek[1,*]

[1] *Physics and Astronomy Department, Michigan State University, East Lansing, Michigan 48824, USA*
[2] *College of Science, Zhejiang University of Technology, Hangzhou 310023, China*

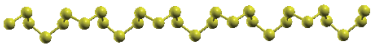

Video 1. MD results of a 4 ps long run for the 1D b-chain at $T = 300$ K.

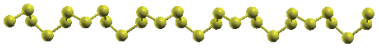

Video 2. MD results of a 4 ps long run for the 1D b-chain at $T = 500$ K.

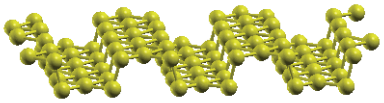

Video 3. MD results of a 2 ps long run for 2D δ-Se at $T = 300$ K.

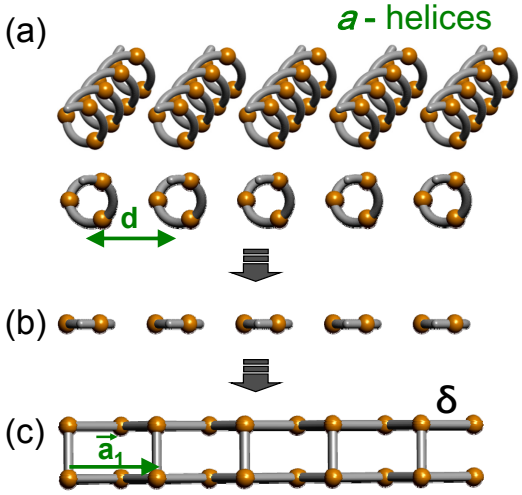

FIG. S1. Transformation of 1D to 2D structures of elemental Se. (a) Perspective and end-on view of the initial 2D assembly of 1D a-chains. (b) End-on view of the structure after artificial confinement to an infinitely thin slab. (c) End-on view of the 2D δ-Se allotrope that formed spontaneously after the structure in (b) was relaxed.

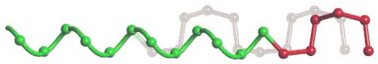

Video 4. Schematic depiction of the a-to-b transformation by dislocation motion.

DYNAMICAL STABILITY OF 1D AND 2D STRUCTURES OF SE

We have performed canonical molecular dynamics (MD) simulations at elevated temperatures to confirm the dynamical stability of the 1D and 2D structures of Se described in the main text. Results of 4 ps long runs for the b-chain are shown in Video 1 for $T = 300$ K and in Video 2 for $T = 500$ K. Results of a 2 ps run for δ-Se at $T = 300$ K are shown in Video 3.

TRANSFORMATION OF 1D TO 2D ALLOTROPES BY ARTIFICIAL CONFINEMENT

As mentioned in the main manuscript, an impractical, yet computationally feasible way to transform 1D to 2D structures is by artificial confinement in a 2D plane, as shown in Fig. S1. The initial structure, depicted in Fig. S1(a), consists of a 2D assembly of parallel Se helices separated by $d = 3.83$ Å. The atomic positions in the artificial flat structure shown in Fig. S1(b) are obtained by projecting this structure onto a plane. By re-optimizing this structure, we obtained 2D δ-Se, shown in Fig. S1(c).

MICROSCOPIC TRANSFORMATION MECHANISM FROM THE δ TO THE η STRUCTURE

The structural transformation from the δ to the η structure is depicted in Fig. S2. The δ allotrope in Fig. S2(a) is transformed to the allotrope in Fig. S2(b) by first reflecting the part of the structure on the right of sites $1, 2, 3$ in a plane containing these atoms. This is to be followed by an infinite series analogous reflections involving sites $4, 5, 6$, then $1', 2', 3'$, etc., resulting in a structure reminiscent of a staircase. The structure in Fig. S2(b) is transformed to the final η allotrope in Fig. S2(c) by an analogous series of reflections. This

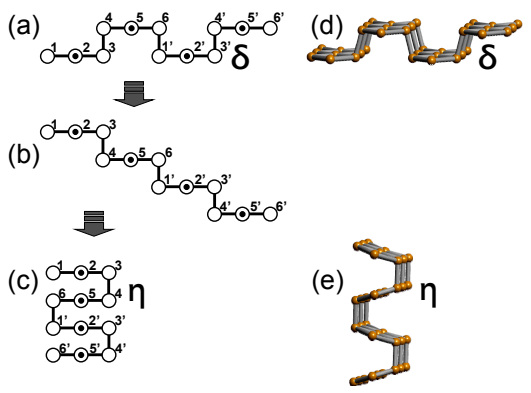

FIG. S2. Structural transformation between the 2D δ and the η allotropes by a series of reflections in planes normal to the picture plane. (a)-(c) Schematic side view of the initial and intermediate structures. Atoms in a plane normal to the lattice are shown by ◯ and atoms in front of these by ⊙. Atoms in one unit cell are labeled by the numbers $1-6$. Primed numbers are used to label atoms in neighboring cells. Perspective views of (d) the initial δ and (e) the final η structure.

transformation starts by reflecting the part of the structure on the right of sites $3, 4$ in a plane containing these atoms. This is to be followed by an infinite series analogous reflections involving sites $6, 1'$, then $3', 4'$, etc. A perspective view of the initial δ structure is shown in Fig. S2(d) and that of the final η structure in Fig. S2(e).

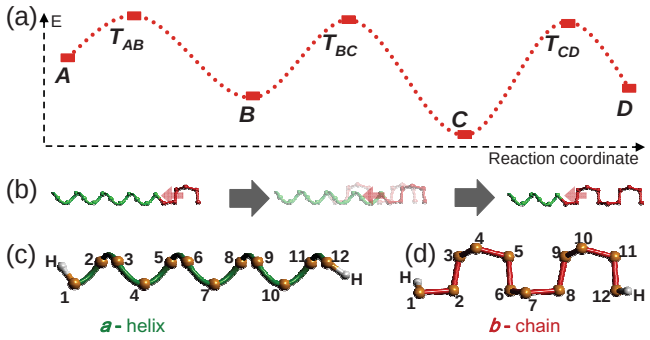

FIG. S3. (Color online) (a) Potential energy E as a function of the optimum reaction coordinate during the A-D transformation. (b) Schematic transformation from the a-helix to the b-chain by dislocation motion, also shown in Video 4. Schematic geometry of hydrogen terminated 9-atom segments of (c) the a-helix and (d) the b-chain. Atoms are labeled for later use.

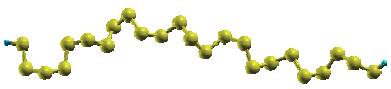

Video 5. MD simulation of the a-to-b transformation.

MICROSCOPIC TRANSFORMATION MECHANISM FROM THE a-HELIX TO THE b-CHAIN

As described in the main text, the most favorable conversion from the infinite a-helix (related to state A) to the more stable b-chain (related to state D) is a multi-state process that involves intermediate states B and C, as indicated in Fig. S3(a). The energetically favored transformation path by dislocation motion along the chain is illustrated schematically in Fig. S3(b) and the corresponding video Video 4. The realistic video Video 5 represents molecular dynamics (MD) results for the optimum transformation path from the A to the D structure. For the following discussion, we label individual atoms by numbers in the finite segment of the a-helix structure in Fig. S3(c) and in the finite segment of the b-chain structure in Fig. S3(d).

Results of selected trajectories from the transition points T, identified in Fig. S3(a), are presented in Figs. S4-S6 in terms of the dihedral angle ψ and the potential energy E as a function of the number of conjugate gradient (CG) steps or as a function of time in MD simulations. We found it very useful to consider both CG and MD calculations. CG optimization reaches the intermediates states only in case that there are no local minima between the transition states T and the adjacent intermediate states. This limitation is eliminated in MD simulations at the cost of large fluctuations in the potential energy E caused by corresponding fluctuations in the kinetic energy, which increases in time. Of course, we found the total energy to be conserved in our microcanonical MD simulations. Inspection of our results in Fig. S4 shows that all trajectories starting in transition point T_{AB}, whether obtained by CG or MD, lead either to the geometry of the adjacent intermediates state A or B. Similarly, in Fig. S5, we found all trajectories from T_{BC} to lead either to state B or C. Finally, as seen in Fig. S6, we found all trajectories from T_{CD} to lead either to state C or the final state D. The potential energy E has been decreasing along all trajectories starting from the frozen transition state geometry.

Interestingly, we found the interatomic bond distances and bond angles to remain near their optimum values during the entire A-D transformation. The third factor associated with stability, the dihedral angle ψ, was found to change significantly during the process. In all transition-state geometries, we could identify 4-atom segments with a very unfavorable dihedral angle ψ near $0°$. Structural evolution of the system from the transition state to the adjacent intermediate state was in all cases accompanied by a change of the particular dihedral angle ψ towards its optimum value $\approx 83°$. As a matter of fact, we could rationalize the entire transformation from A to D by a sequence of bond rotations.

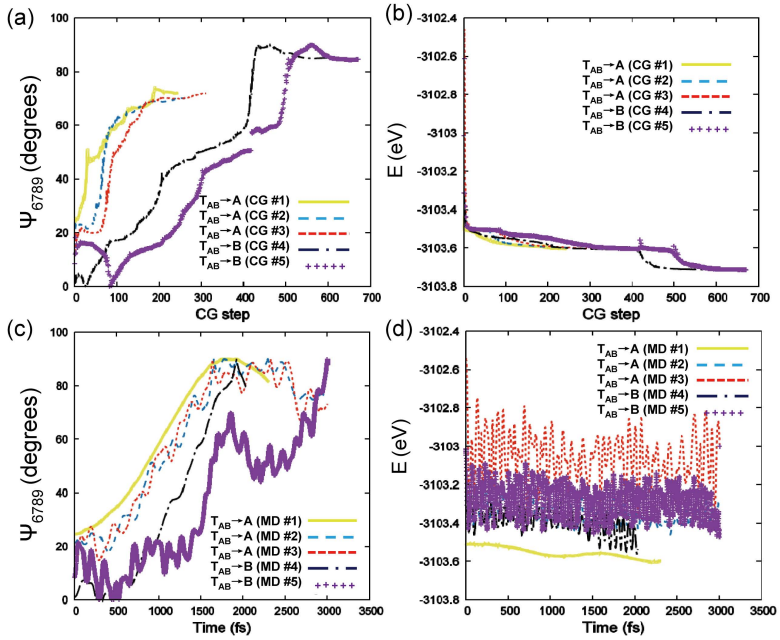

FIG. S4. (Color online) (a,c) Dihedral angle ψ and (b,d) potential energy E of the Se system during (a,b) CG optimization and (c,d) MD calculations starting in transition point T_{AB}, identified energetically in Fig. S3(a). Atomic positions used to define ψ_{6789} are identified in Fig. S3(c) and S3(d).

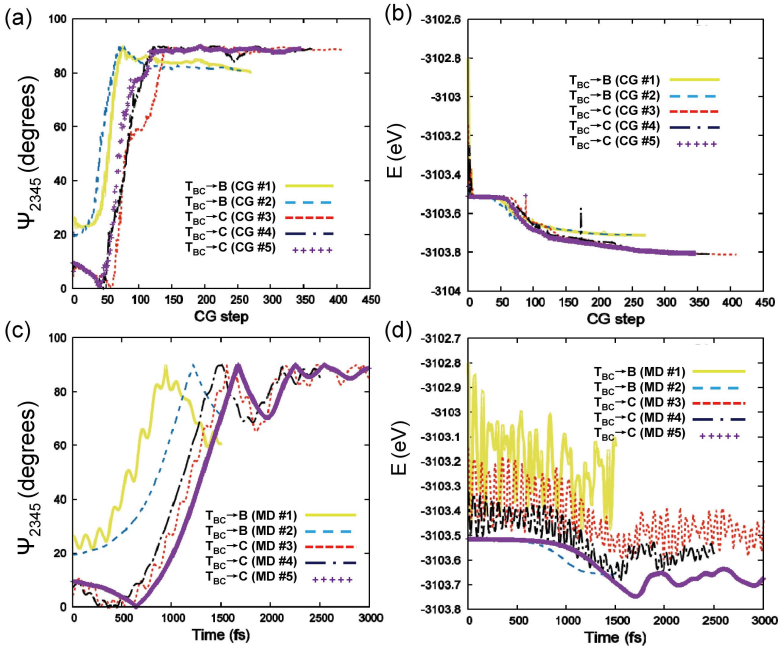

FIG. S5. (Color online) (a,c) Dihedral angle ψ and (b,d) potential energy E of the Se system during (a,b) CG optimization and (c,d) MD calculations starting in transition point T_{BC}, identified energetically in Fig. S3(a). Atomic positions used to define ψ_{2345} are identified in Fig. S3(c) and S3(d).

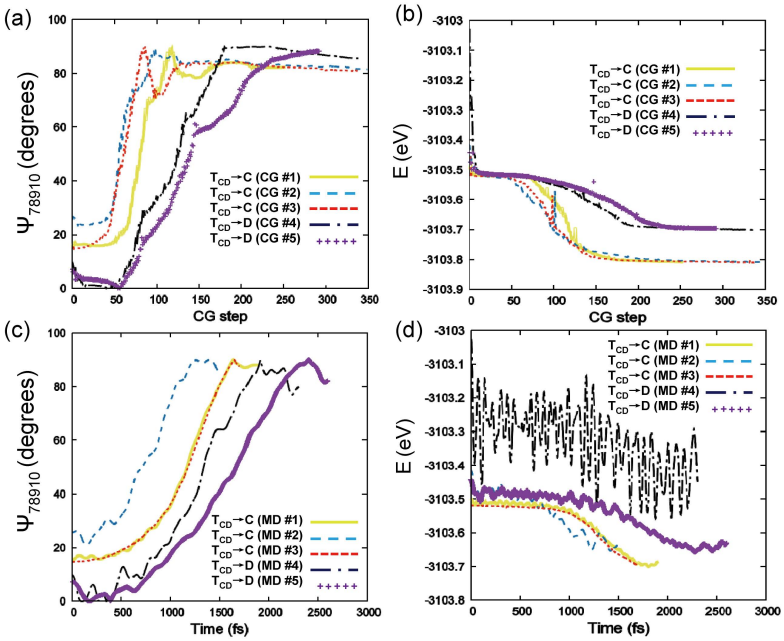

FIG. S6. (Color online) (a,c) Dihedral angle ψ and (b,d) potential energy E of the Se system during (a,b) CG optimization and (c,d) MD calculations starting in transition point T_{CD}, identified energetically in Fig. S3(a). Atomic positions used to define $\psi_{789,10}$ are identified in Fig. S3(c) and S3(d).

* tomanek@pa.msu.edu